**Nationaal Lucht- en Ruimtevaartlaboratorium**

National Aerospace Laboratory NLR


NLR-TP-99108

# Source location by phased array measurements in closed wind tunnel test sections

P. Sijtsma and H. Holthusen

**Nationaal Lucht- en Ruimtevaartlaboratorium**

National Aerospace Laboratory NLR

NLR-TP-99108

# Source location by phased array measurements in closed wind tunnel test sections

P. Sijtsma and H. Holthusen*

* *German Dutch Wind Tunnel DNW*

The contents of this report have been initially prepared for publication as AIAA paper 99-1814 in the Proceedings of the 5th AIAA/CEAS Aeroacoustics Conference, Greater Seattle, Washington, USA, 10-12 May 1999.



| | |
|---|---|
| Division: | Fluid Dynamics |
| Issued: | 8 March 1999 |
| Classification of title: | Unclassified |

## Contents

**I. Introduction** 3

**II. Array design** 4
Microphone set-up 4
Reduction of boundary layer noise 4

**III. Assessment of wall effects** 5

**IV. Airframe noise measurements** 5
The effect of the porous layer 5
Third octave-band results 6
Strouhal cylinders 6

**V. Conclusion** 6

**References** 7

25 Figures

(13 pages in total)

AIAA-99-1814

# Source Location by Phased Array Measurements in Closed Wind Tunnel Test Sections

Pieter Sijtsma*
*National Aerospace Laboratory NLR, 8300 AD Emmeloord, The Netherlands*
and
Hermann Holthusen†
*German Dutch Wind Tunnel DNW, 8300 AD Emmeloord, The Netherlands*

**The feasibility of high frequency phased array measurements on aircraft scale models in a closed wind tunnel test section was investigated. For that purpose, 100 microphones were built in a 0.6×0.5 $m^2$ plate, which was installed in a floor panel of the 8×6 $m^2$ test section of the Large Low-speed Facility of the German Dutch Wind tunnel (DNW-LLF). For the microphone positions a sparse array design was used that minimises side lobes in the beamforming process. To suppress boundary layer noise, the array could optionally be covered with a 0.5 cm thick layer of acoustic foam and a 5% open perforated plate. To assess the effect of wall reflections, tests without wind were performed with a loudspeaker at several positions in the tunnel section. Furthermore, wind tunnel tests were carried out on an Airbus transport aircraft model. It is shown that location of acoustic sources is indeed possible for frequencies between 2 and 30 kHz, but their levels may differ from those measured in an anechoic environment. For the lower frequencies, application of the layer of foam and the perforated plate is beneficial. Finally, it is shown that filtering out the most dominant source can extend the array potential.**

## I. Introduction

Microphone arrays or acoustic antennas become more and more in use as a wind tunnel measurement tools to locate sound sources (Refs. 1-5). Microphone arrays have the advantage over acoustic mirrors of a higher measurement speed. Mirrors have to scan the whole test object, while microphone arrays only need a short time to record signals. The process of scanning through possible source locations is performed afterwards by appropriate software. The increasing capacity of computers and data acquisition systems enables the use of a large number of microphones. Herewith the traditional drawback of microphone arrays compared to acoustic mirrors, namely the lower spatial resolution, is getting compensated.

An additional advantage of a microphone array is the application inside the flow or in the wall of a closed test section. These in-flow measurements with a microphone array are possible, provided that turbulent self-noise of the array is suppressed sufficiently. With a mirror, in-flow measurements are evidently impossible.

In the present tests, an array of 100 microphones was mounted in the floor of the 8×6 $m^2$ test section of the Large Low-speed Facility of the German Dutch Wind Tunnel DNW (Fig. 1). A sparse array design was used in order to minimise spatial side lobes (Ref. 6). The purpose of the array is to locate airframe noise sources on scale models of transport aircraft and therefore it should be able to locate sources at frequencies up to 30 kHz.

The microphones have been mounted flush in a plate of the same width as a floor panel of the standard test section, so that it can be installed and removed easily. Installation in a side wall panel is also possible. To suppress the boundary layer noise, the array plate can

* Research Engineer, Aeroacoustics Department, P.O. Box 153, Email: sijtsma@nlr.nl.
† P.O. Box 175, Email: holthuse@nlr.nl.

optionally be covered with a 0.5 cm thick layer of acoustic foam and a 5% open perforated plate.

An important phenomenon, which may devaluate acoustic measurements in a closed test section, is the effect of wall reflections. As a result, source levels may be found which are different from corresponding levels in an open environment. In order to study this effect, no-wind measurements were carried out with a loudspeaker at several positions and comparisons were made to measurements under anechoic conditions. It appeared that conclusions with respect to the source levels have to be made carefully and that acoustic sources should not be too close to a wall.

To investigate the array's ability to locate airframe noise sources and to establish the merits of the porous layer (foam and perforated plate), measurements were carried out on an Airbus transport aircraft model (scale 1:10) with high lift devices. Airframe noise sources were observed in the frequency range 2-30 kHz and the porous layer appeared useful for frequencies up to approximately 8000 Hz. With Strouhal cylinders attached to the model, it was demonstrated that the array processing software is able to locate the sources with high precision.

In this paper a brief discussion is given on the design of the array (microphone locations and porous layer). Then, some results are shown of the speaker measurements. Further, the airframe noise measurements will be discussed. Finally, it is demonstrated that the array gain (difference between main lobe and highest side lobe) can be enlarged by filtering out the dominant source (Ref. 7).

## II. Array design

**Microphone set-up**

The 100 microphones were mounted in a 0.6×0.5 $m^2$ plate. An irregular, sparse array design was used. The microphone set-up, shown in Fig. 2, was chosen such that, for a large frequency range, maximum side lobe suppression is reached for a conventional beamforming technique (Ref. 8). This optimisation is carried out as follows.

Ideally, the acoustic pressure $p$ in the microphone plane $z = z_0$ is known everywhere, but in reality it is known only in a finite number of points, viz. the microphone positions $(x_k, y_k)$. The measured pressure $p_{\text{meas}}$ can formally be described by

$$p_{\text{meas}}(x, y) = \sum_{k=1}^{N} p(x_k, y_k)\delta(x - x_k, y - y_k), \qquad (1)$$

where $\delta$ is the Dirac-delta function and $N$ is the number of microphones. In the wave number domain we have

$$P_{\text{meas}}(\alpha, \beta) = P(\alpha, \beta) * W(\alpha, \beta), \qquad (2)$$

where $*$ denotes convolution and $W$ is the "aperture smoothing function" (Ref. 8), given by:

$$W(\alpha, \beta) = \sum_{k=1}^{N} \exp\left(-i(\alpha x_k + \beta y_k)\right). \qquad (3)$$

Now suppose $P$ has a peak value at $(\mapsto_1, \updownarrow_1)$ and $W$ has a peak value at $(\mapsto_2, \updownarrow_2)$. Then from Eq. 2 it follows that $P_{\text{meas}}$ has a peak at $(\mapsto_1+\mapsto_2, \updownarrow_1+\updownarrow_2)$. Therefore, peak values of $W$ outside (0,0) cause dispersion to spurious sources. Low dispersion can be obtained when the following integral is minimised as a function of microphone locations $(x_k, y_k)$:

$$\iint_{k_{\min}^2 < \alpha^2 + \beta^2 < k_{\max}^2} |W(\alpha, \beta)|^2 \, d\alpha d\beta \qquad (4)$$

The bounds $k_{\min}$ and $k_{\max}$ depend on array diameter and maximum frequency, respectively.

Based on the optimisation described above, under the constraints of the plate dimensions and a minimum distance between microphones, the array set-up has been designed. Two subsets of 68 microphones can be defined: one for low frequency (2-12 kHz) and one for high frequency (10-30 kHz) measurements. With these settings, a theoretical array gain (difference between main lobe and highest side lobe) of more than 12 dB up to 10 kHz was achieved and approximately 10 dB for higher frequencies. These results are comparable to those in reference 9.

**Reduction of boundary layer noise**

As stated in the introduction, the option was included to cover the array plate with a layer of acoustic foam and a perforated plate. The idea behind this is that a layer of porous material suppresses the turbulent boundary layer noise much more than noise from a stationary source, because of the small wave lengths in the boundary layer (e.g. Ref. 10).

It was chosen to use a 0.5 cm thick layer of foam and a 5% open perforated plate. A thickness of 0.5 cm seemed to be enough to suppress the boundary layer noise considerably in the frequency range of interest: 2-8 kHz. The attenuation of the turbulent boundary

layer noise through the porous layer depends on the wave lengths of the hydrodynamic distortions and is exponential with layer thickness. An estimation of the frequency dependent transmission loss through the 0.5 cm thick porous layer is shown in Fig. 3.

As shown in Fig. 4, the combination of the 0.5 cm of acoustic foam with the 5% open perforated plate does not seem to distort the noise from a stationary source too much. The transmission loss remains limited to a few dB and almost independent of the angle of incidence between 45° en 135°.

The results of Fig. 4 were calculated for Mach number $M = 0.2$, when, according to reference 11, the resistance of the perforated plate is $Z \approx 1.2\rho c$. The transmission of sound through the acoustic foam was calculated with a simple model for sound propagation through porous materials, as in reference 12.

Also seen in Fig. 4 is that unwanted noise from outside the view angle is strongly attenuated. This is an additional advantage of the porous layer.

For high frequencies, say higher than 8 kHz, the application of the porous layer (plate & foam) may not be needed anymore because of the rapid fall-off of the boundary layer noise spectrum (e.g. Ref. 13)

## III. Assessment of wall effects

Tests were performed with a loudspeaker installed in the test section (without wind) to investigate the effect of wall reflections. Using a conventional beamforming algorithm, it appeared that the speaker locations could be retraced correctly in the frequency range of interest. In other words, wall reflections had no influence on the ability to recover source locations.

To show the effect of wall reflections on the source strengths, we consider a series of array measurements without porous layer, with the speaker at 3 m above the array plate. In this series, the speaker is located in the same tunnel cross section area as the array centre (say $x = 0$). The transverse co-ordinate ($y$) had the values $y = 0.07$, $y = 1.07$, $y = 2.73$ and $y = 3.25$, where the tunnel centre is assumed to be at $y = 0$. In other words, the first position is almost on the tunnel centre line. The array centre is located at $y = 1.07$, hence the second position is just above the array. The fourth position is only 75 cm from the wall.

A point of concern is the possible influence of wall reflections on the source characteristics. In other words, the actual source strength of the speaker may be dependent of its position. This is checked with a reference microphone at 25 cm from the source. The signals of the reference microphone at the several speaker positions are shown in Fig. 5. It is clear that the influence of position of the speaker on its characteristics is negligible.

Next, the source strengths found by beamforming were compared to measurements in an anechoic chamber. These anechoic measurements were carried out with a single microphone at 2 m distance at several angles. For a good comparison, the beamforming results were also transformed into acoustic levels at 2 m from the source. Results of the comparison are shown in Fig. 6 through Fig. 9.

It can be seen that the agreement is reasonable, but narrow-band differences up to 5 dB are possible. To obtain more acceptable agreement, the results should be presented in a third octave-band spectrum. When the speaker approaches the wall, the low frequency results are more and more polluted by interference (Fig. 8, Fig. 9).

## IV. Airframe noise measurements

The possibilities of the application of the microphone array in the $8 \times 6$ m$^2$ test section were investigated further during aerodynamic measurements on two Airbus transport aircraft models with high lift devices. Array measurements were carried out with high frequency and low frequency microphone setting, with and without porous layer.

The position of the array with respect to the model is shown in Fig. 10. The model was located at mid-height, in other words, 3 m above the array. Most measurements were carried out at Mach number $M = 0.2$.

The array measurements were carried out for a limited number of configurations, without a systematic research on the effect of different model settings (flap angles, etc.).

**The effect of the porous layer**

For a number of low frequency array measurements, in Fig. 11 results are plotted of mean array auto-power, with and without porous plate. When we compare the result with and without porous layer to each other, the following can be observed.

Up to 2000 Hz, the difference between the layer and the no-layer results increases. At 2000 Hz the

difference is approximately 13 dB, which is the same as the predicted transmission loss of turbulent boundary layer noise (Fig. 3). From 2000 Hz to 5000 Hz, the difference slowly decreases and above 5000 Hz, the difference remains more or less constant.

It looks as if the array auto-powers are dominated by boundary layer turbulence up to 2000 Hz for the array with porous layer and up to 5000 Hz for the array without porous layer. Unfortunately, there was no opportunity to perform measurements with flow in an empty test section to verify this.

An indirect way of verifying the assumption that boundary layer noise dominates up to 5000 Hz is to compare with wall pressure measurements shown by Blake in reference 13, fig. 8-41. In Fig. 12, array measurements without porous layer are presented in the same way as by Blake. Here, $\Phi_{pp}$ is the auto-correlation function (auto-power when $\Delta f = 0$), $\rho$ is the air density, $U$ is the tunnel speed and $\delta^*$ is the displacement thickness of the boundary layer (approximately 2 cm). The results in Fig. 12 follow well the results of Blake, fig. 8-41. But for $2\pi f\delta^*/U > 10$, which corresponds to $f > 5400$ Hz, the DNW results are significally higher than Blake's results.

In Fig. 13 and Fig. 14 results of acoustic scans at 3000 Hz, narrow-band ($\Delta f = 50$ Hz), are shown without and with porous layer, respectively. For the no-layer case in Fig. 13 it is seen that acoustic sources on the aircraft model can be found, despite the fact that the microphone signals are dominated by boundary layer noise. However, also spurious sources are found outside the model. In Fig. 14, where the porous layer has been applied, the scan looks much "cleaner".

**Third octave-band results**

Another way to get rid of spurious sources is to look at the third octave-band spectrum. Then a number of narrow-band results have to be summed. For each narrow-band frequency, the spurious sources appear on different location, while the physical sources stay on the same spot. This is demonstrated in Fig. 15, which shows the results at 3150 Hz, third octave-band, for the same measurements as in Fig. 13.

In Fig. 16 through Fig. 18, third octave-band results are shown at 2500, 6300 and 12500 Hz. This shows the frequency range, at which reasonable results are found with the low frequency array. With the high frequency array, good third octave-band results were found between 8000 Hz (Fig. 19) and 25000 Hz (Fig. 21). In Fig. 20 also the result is shown at 16000 Hz. At 31500 Hz (Fig. 22), sources on the aircraft model can still be recognised, although their levels are not higher anymore than those of some spurious sources.

**Strouhal cylinders**

During part of the tests, at several positions on the aircraft model small cylinders were attached, pointing horizontally and perpendicular to the flow, in order to generate Strouhal tones. This was to check the ability of the array software to find the acoustic sources on the right spot.

Measurements showed that this was indeed the case. This can be seen, for example, in Fig. 23 and Fig. 24, which are narrow-band results at 6671 Hz and 7031 Hz, respectively, derived from measurements with the low frequency array and the porous layer. On the inner engine nacelle one cylinder was attached, pointing towards the fuselage. On the outer nacelle, two cylinders were attached, one pointing towards the fuselage, the other pointing in the opposite way. In the above-mentioned figures, sound sources are indeed found on these locations.

Although these cylinders had identical diameter, the outer most cylinder produced a tone at a frequency slightly higher than the other two, probably due to local flow differences.

When one source is dominant, as in Fig. 24, we can improve the array gain by filtering it out. This can be done by eigenvalue analysis, viz. removing from the cross-power matrix the eigenvector corresponding to the highest eigenvalue (see Ref. 7). The result, at the same frequency as in Fig. 24 is seen in Fig. 25, where the Strouhal source has disappeared and other sources, e.g. on the trailing edge flaps, become visible.

## V. Conclusion

A new acoustic array, which can be mounted in the floor of a closed wind tunnel test section, was tested. Measurements with a loudspeaker showed that source levels may be affected by wall reflection, but if the results are presented in third octave-band spectra and if the sound source is not too close to the wall, the accuracy of the source levels found by beamforming is acceptable.

Airframe noise measurements on a 1:10 scale Airbus model showed that sources could be found at expected locations. The array proved to be capable of filtering out the turbulent self-noise. Application of a

Measurements with a loudspeaker showed that source levels may be affected by wall reflection, but if the results are presented in third octave-band spectra and if the sound source is not too close to the wall, the accuracy of the source levels found by beamforming is acceptable.

Airframe noise measurements on a 1:10 scale Airbus model showed that sources could be found at expected locations. The array proved to be capable of filtering out the turbulent self-noise. Application of a porous layer (0.5 cm foam, covered by a 5% open perforated plate) in order to reduce turbulent boundary layer noise showed to be beneficial for frequencies lower than 8000 Hz. Further, it was shown that the array gain can be enlarged by filtering out a dominant source.

## Acknowledgement

The authors are grateful to Daimler Chrysler Aerospace Airbus for giving the opportunity to perform the acoustic measurements.

## References

1. Hayes, J.A.; Horne W.C.; Soderman, P.T.; Bent, P.H., Airframe noise characteristics of a 4.7% scale DC-10 model, AIAA paper 97-1594, 1997.
2. Meadows, K.R.; Brooks, T.F.; Humphreys, W.M.; Hunter, W.H.; Gerhold, C.H., Aeroacoustic measurements of a wing-flap configuration, AIAA Paper 97-1595, 1997.
3. Dobrzynsky, W.D.; Buchholtz, H., Full-scale noise testing on airbus landing gears in the German-Dutch Wind Tunnel, AIAA Paper 97-1597, 1997.
4. Piet, J.F.; Elias, G., Airframe noise source localization using a microphone array, AIAA Paper 97-1643, 1997.
5. Dassen, A.G.M.; Sijtsma, P.; Holthusen, H.H.; Haaren, E. van; Parchen, R.R.; Looijmans, K.N.H., The noise of a high-speed train pantograph as measured in the German-Dutch Wind Tunnel DNW, presented at the 2nd International Workshop on the AeroAcoustics of High-Speed Trains, Berlin, 29/30 April 1997.
6. Sijtsma, P., Optimum arrangements in a planar microphone array, presented at the First CEAS-ASC Workshop: Wind Tunnel Testing in Aeroacoustics, DNW, 5/6 November 1997.
7. Dougherty, R.P., Source Location with Sparse Acoustic Arrays; Interference Cancellation, presented at the First CEAS-ASC Workshop: Wind Tunnel Testing in Aeroacoustics, DNW, 5/6 November 1997.
8. Johnson, D.H.; Dudgeon, D.E., Array Signal Processing, Prentice Hall, 1993.
9. Underbrink, J.R.; Dougherty, R.P, Array design of non-intrusive measurement of noise sources, Noise-Con 96, Seattle, Washington, 29 September-2 October 1996.
10. Maidanik, G., Domed sonar system, Journal of the Acoustical Society of America, Vol. 44, No. 1, 1968, pp. 113-124.
11. Guess, A.W., Calculation of perforated plate liner parameters from specified acoustic resistance and reactance, Journal of Sound and Vibration, Vol. 40, No. 1, 1975, pp. 119-137.
12. Nayfey, A.H.; Kaiser, J.E.; Telionis, D.P., Acoustics of aircraft engine-duct systems, AIAA Journal, Vol. 13, No. 2, 1975, pp. 130-153.
13. Blake, W.K., Mechanics of Flow-Induced Sound and Vibration, Vol. II, Complex Flow-Structure Interactions, Academic Press, 1986.

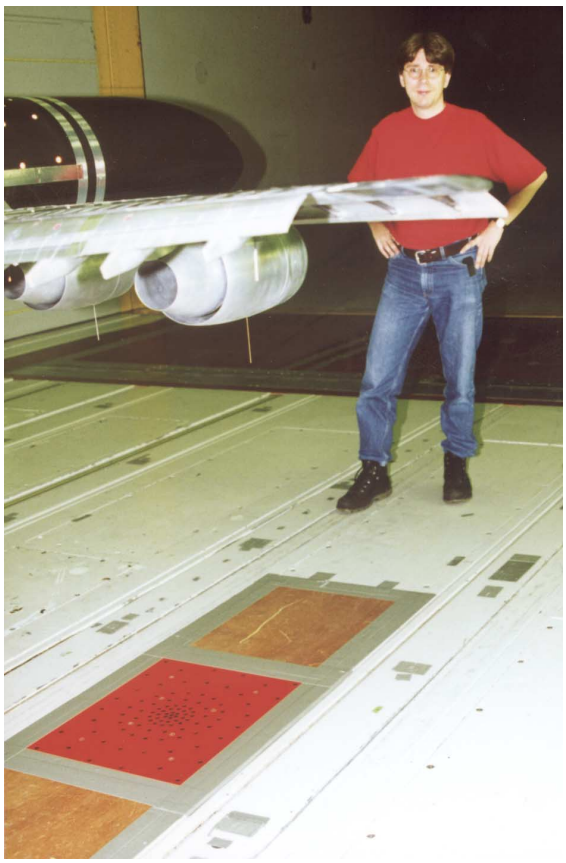

Fig. 1 DNW floor array

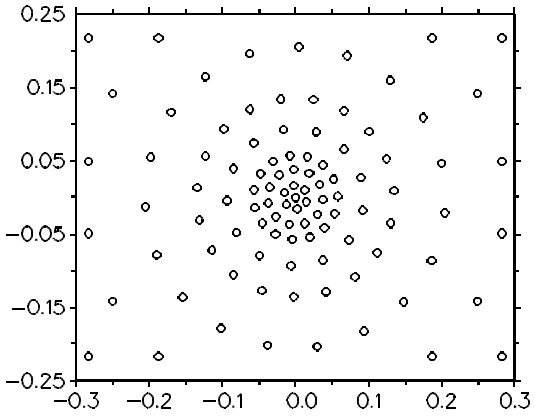


Fig. 2 Microphone set-up (units in m.)

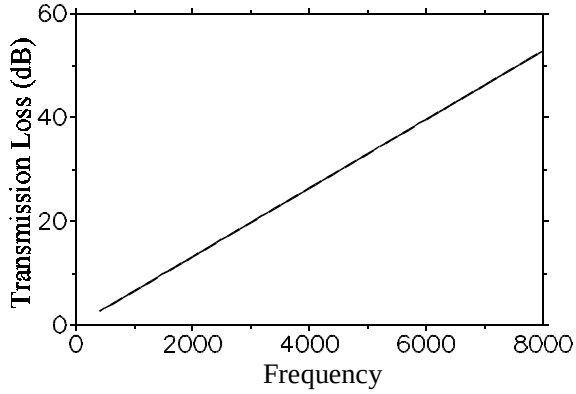


Fig. 3 Transmission loss over porous layer of turbulent boundary layer noise

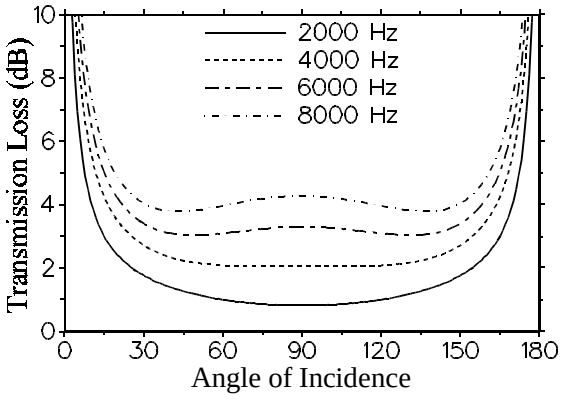


Fig. 4 Transmission loss over porous layer of noise from stationary source

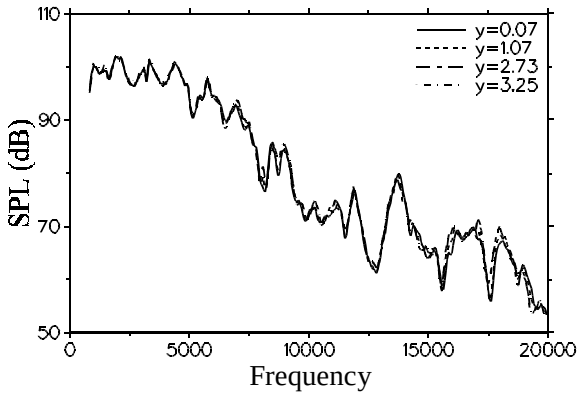


Fig. 5 Signal strengths of reference microphone at several speaker locations

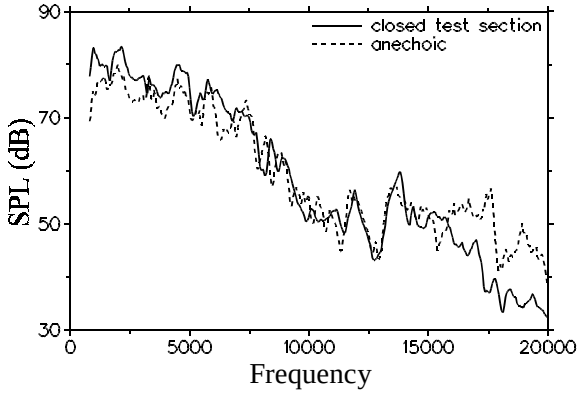


Fig. 6 Array measurements compared to anechoic measurements at 2 m from the source, $y$ = 0.07

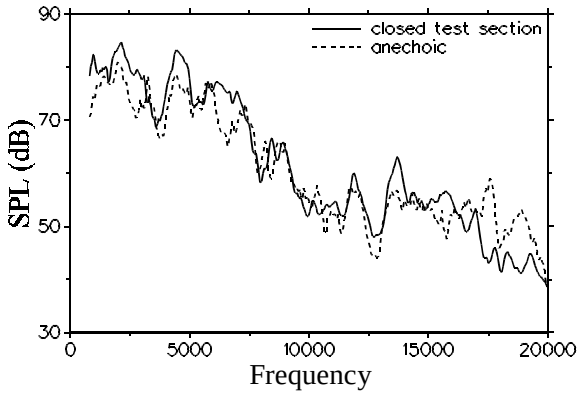


Fig. 7 Array measurements compared to anechoic measurements at 2 m from the source, $y$ = 1.07

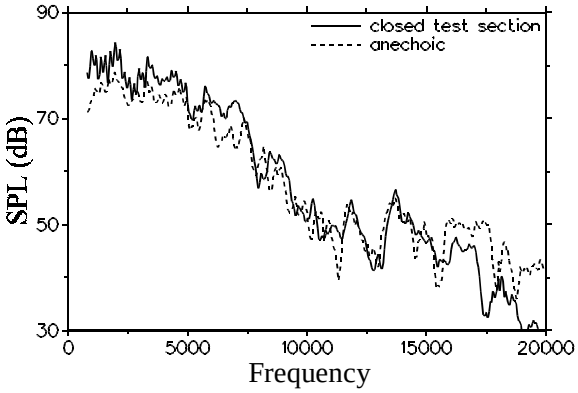


Fig. 8 Array measurements compared to anechoic measurements at 2 m from the source, $y$ = 2.73

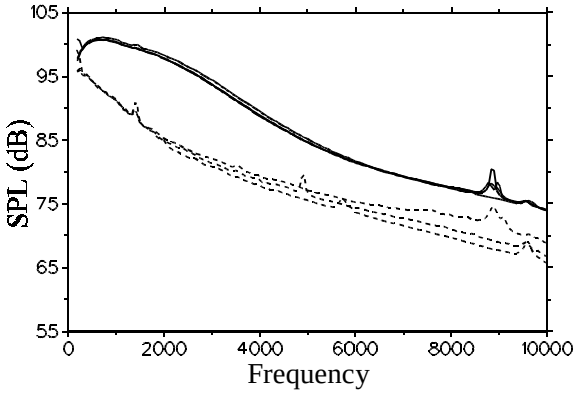


Fig. 11 Several measurements of microphone array auto-power; solid lines: without porous layer, dashed lines: with porous layer

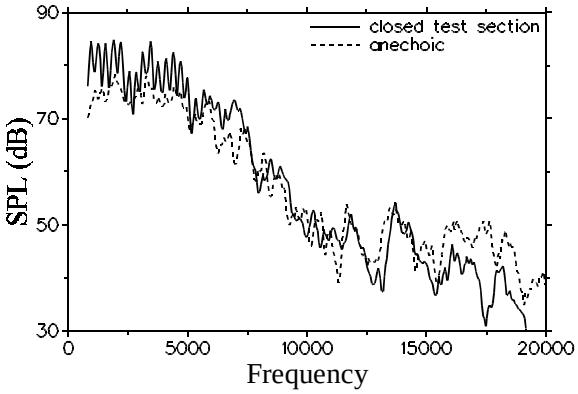


Fig. 9 Array measurements compared to anechoic measurements at 2 m from the source, $y$ = 3.25

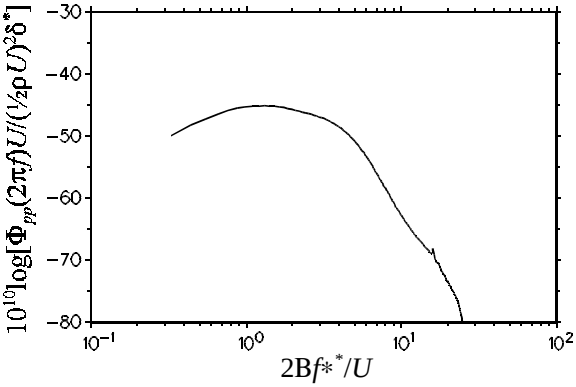


Fig. 12 Microphone array auto-power measured without porous layer, scaled as in Ref. 13, fig. 8-41

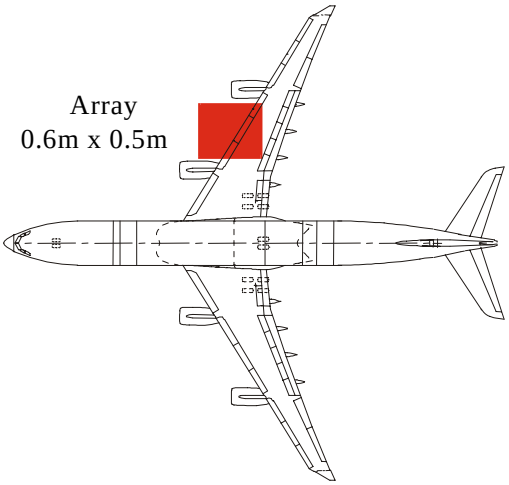


Fig. 10 Position of the array

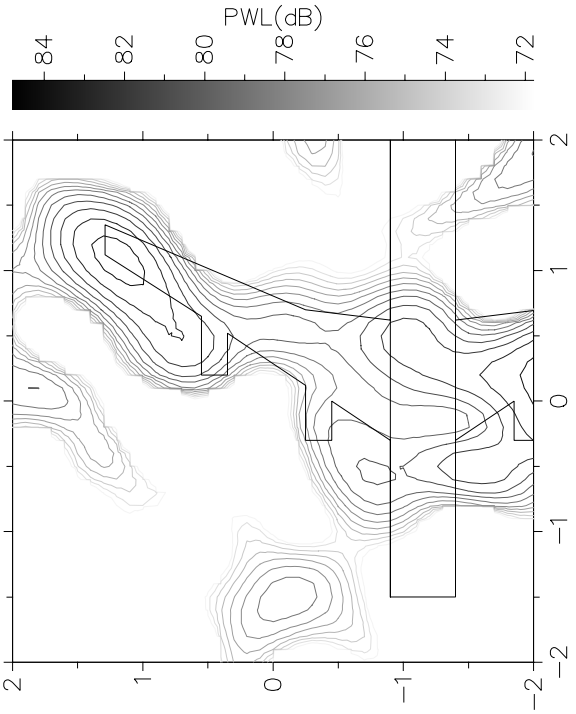


Fig. 13 Acoustic scan without porous layer, 3000 Hz, narrow-band, low frequency array (dimensions in m.)

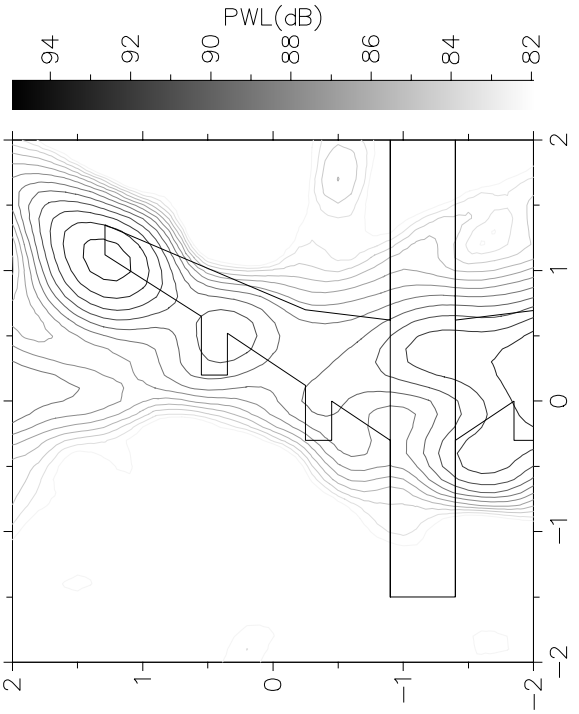


Fig. 15 Acoustic scan without porous layer, 3150 Hz, third octave-band, low frequency array (dimensions in m.)

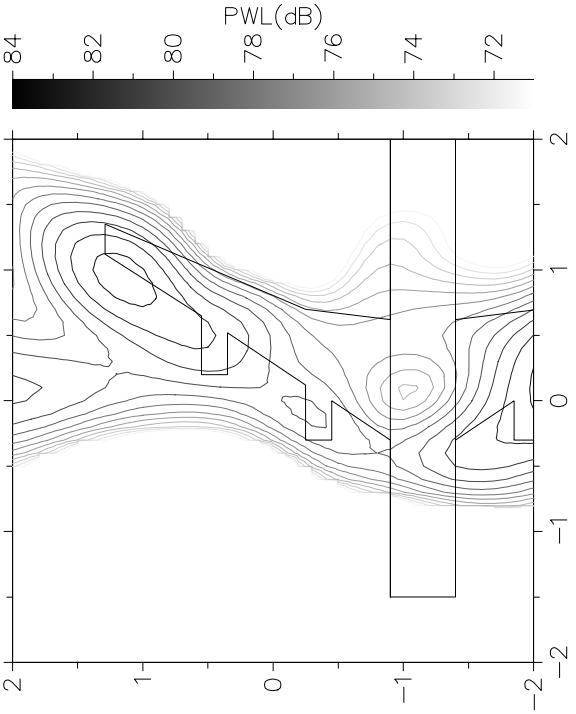


Fig. 14 Acoustic scan with porous layer, 3000 Hz, narrow-band, low frequency array (dimensions in m.)

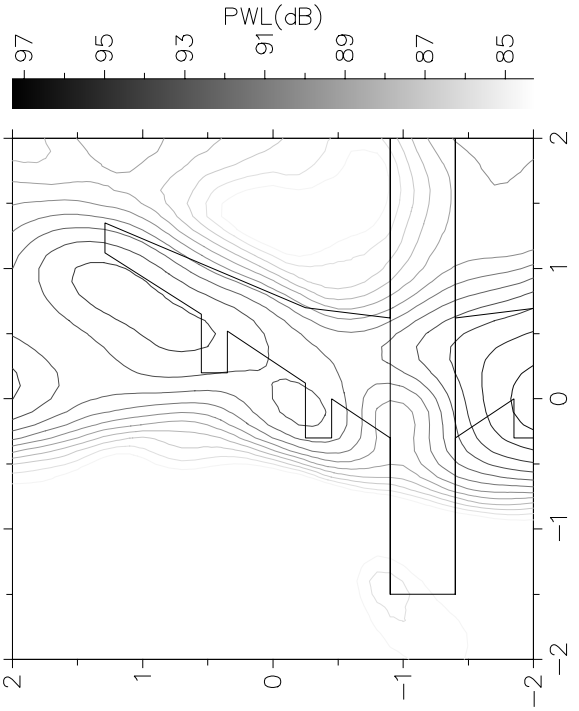


Fig. 16 Acoustic scan without porous layer, 2500 Hz, third octave-band, low frequency array (dimensions in m.)

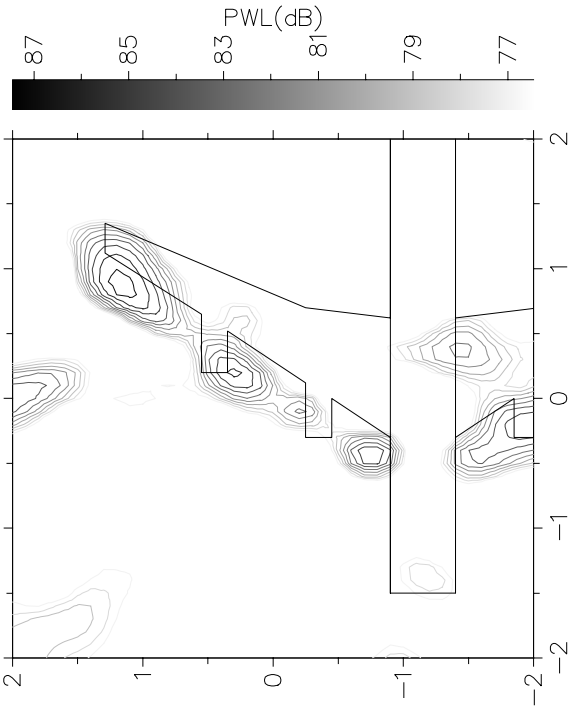


Fig. 17 Acoustic scan without porous layer, 6300 Hz, third octave-band, low frequency array (dimensions in m.)

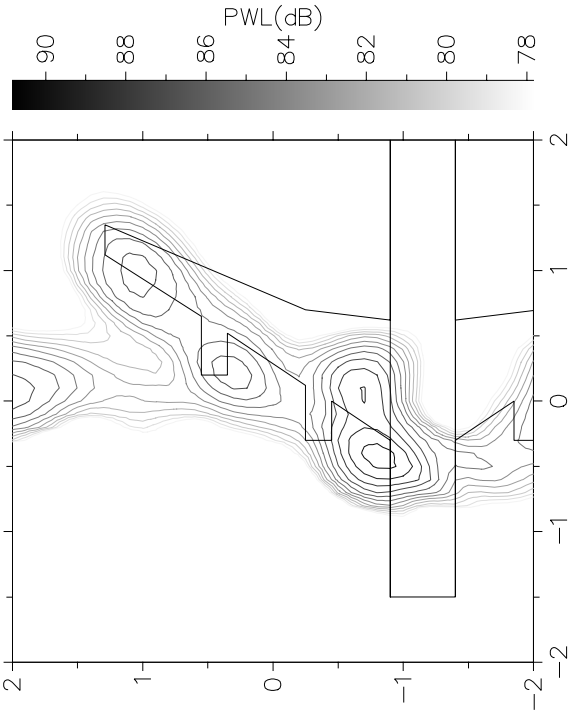


Fig. 19 Acoustic scan without porous layer, 8000 Hz, third octave-band, high frequency array (dimensions in m.)

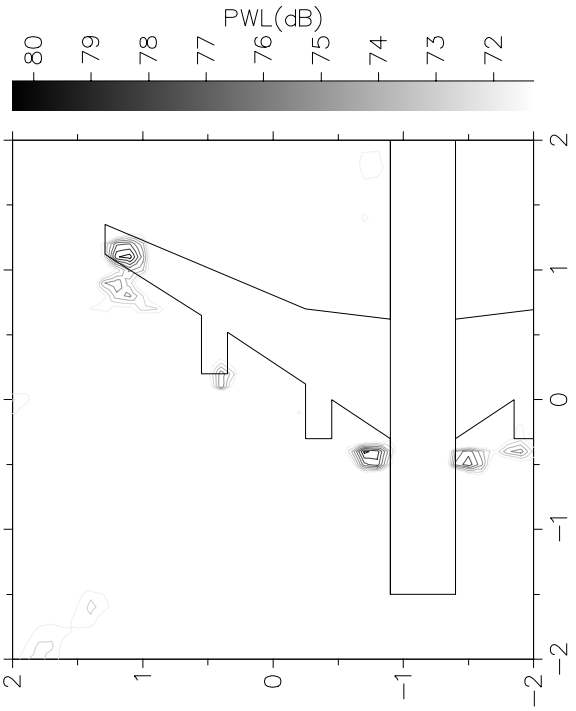


Fig. 18 Acoustic scan without porous layer, 12500 Hz, third octave-band, low frequency array (dimensions in m.)

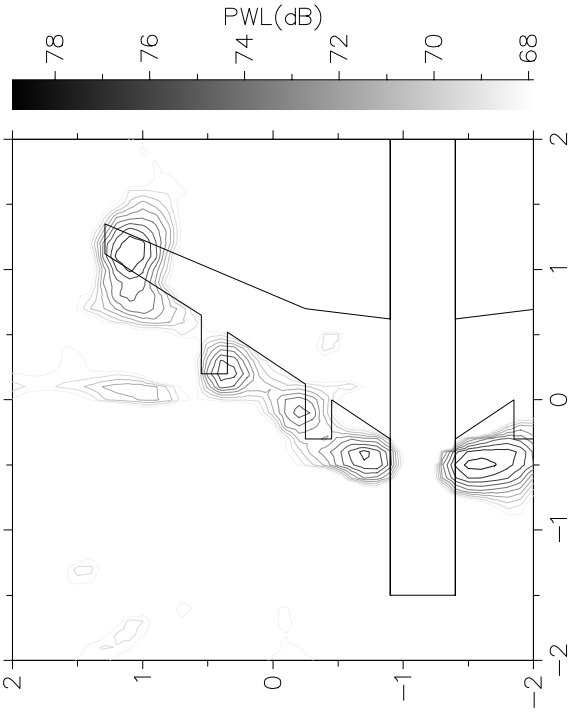


Fig. 20 Acoustic scan without porous layer, 16000 Hz, third octave-band, high frequency array (dimensions in m.)

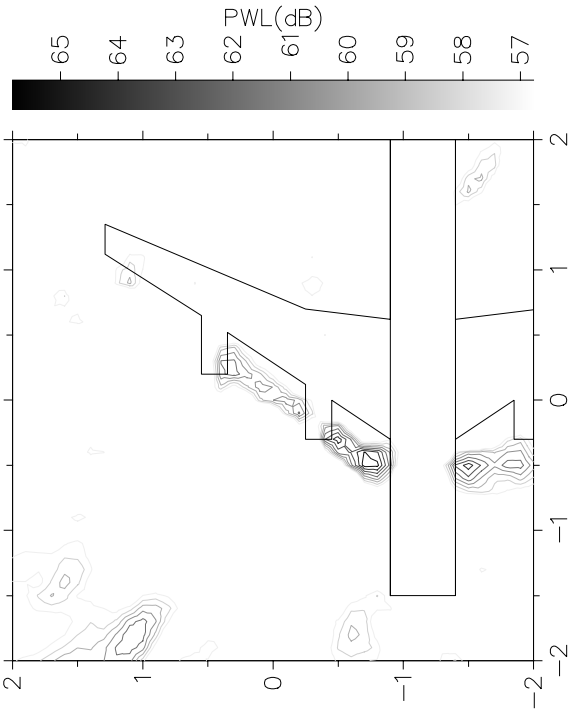


Fig. 21 Acoustic scan without porous layer, 25000 Hz, third octave-band, high frequency array (dimensions in m.)

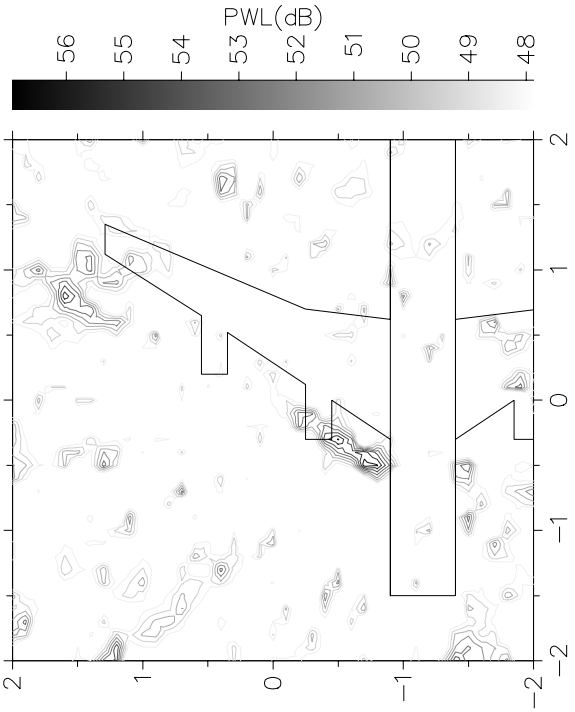


Fig. 22 Acoustic scan without porous layer, 31500 Hz, third octave-band, high frequency array (dimensions in m.)

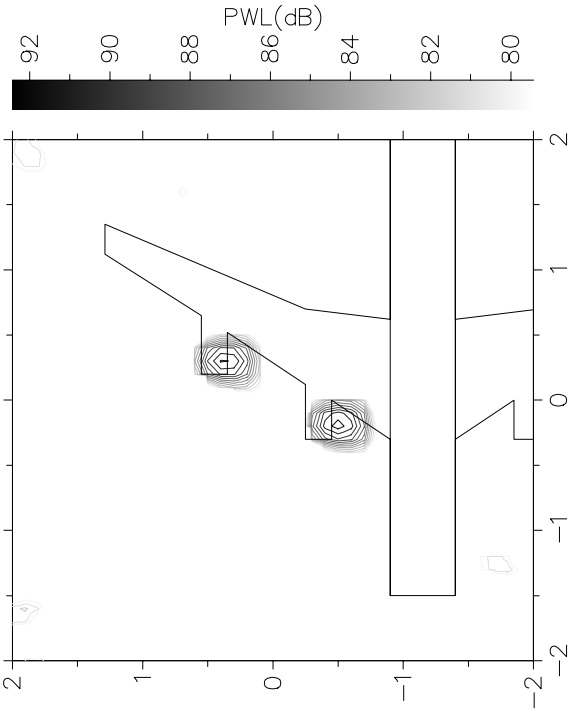


Fig. 23 Acoustic scan with porous layer, 6671 Hz, narrow-band, low frequency array (dimensions in m.)

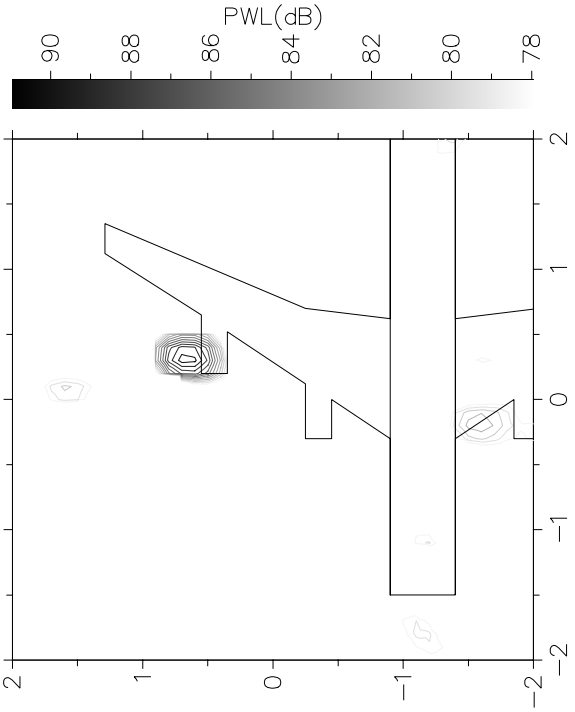


Fig. 24 Acoustic scan with porous layer, 7031 Hz, narrow-band, low frequency array (dimensions in m.)

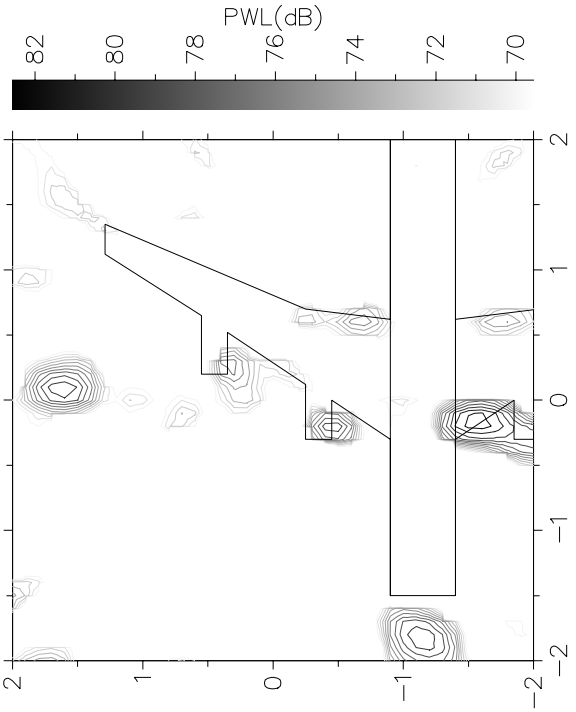


Fig. 25 Acoustic scan with porous layer after filtering out the dominant source, 7031 Hz, narrow-band, low frequency array (dimensions in m.)